Formation energies, binding energies, structure, and electronic transitions of Si divacancies studied by density functional calculations

R. R. Wixom and A. F. Wright
Sandia National Laboratories, Albuquerque, New Mexico 87185, USA
(Received 22 August 2006; revised manuscript received 27 September 2006; published 21 November 2006)

Atomic configurations, formation energies, electronic transition energies, and binding energies of the silicon divacancy in the +1, 0, −1, and −2 charge states were obtained from density functional theory calculations. The calculations were performed using the local density approximation (LDA) and also the Perdew, Burke, Ernzerhof (PBE) formulation of the generalized-gradient approximation. Supercells of nominally 216, 512, and 1000 atoms were used to extrapolate formation energies for infinite-sized supercells corresponding to isolated defects. The predicted ground-state configuration was found to depend on charge state and the chosen formulation of exchange and correlation (LDA or PBE). Structures, binding energies, and transition energies are compared to values reported in the literature.

DOI: 10.1103/PhysRevB.74.205208 PACS number(s): 61.72.Ji, 61.72.Bb, 71.55.Cn

I. INTRODUCTION

The Si divacancy (VV_{Si}) has been a subject of research for over 40 years and as a result, the electronic properties are generally understood. It is interesting however, that there is still considerable disagreement concerning the ground-state atomic configuration. The early electron paramagnetic resonance (EPR) work of Watkins and Corbett[1,2] characterized the structure of the singly charged (+ or −) VV_{Si} as a large-pairing (LP) Jahn-Teller distortion with C_{2h} symmetry. Saito and Oshiyama, using density functional theory (DFT), corroborated the LP structure for the singly positive VV_{Si}, but for the singly negative VV_{Si} they proposed a new resonant-bond (RB) structure that also has C_{2h} symmetry.[3] Another theoretical study by Seong and Lewis also predicts the RB structure for the neutral VV_{Si}.[4] These early theoretical findings are not entirely consistent with the experimental observations and they have been contradicted by more recent density functional calculations that used larger supercells and different formulations of exchange and correlation. Pesola and co-workers[5] report a low-symmetry S_2 configuration (mixed LP and RB character) and Öğüt and Chelikowsky[6] report the LP configuration for the positive, neutral, and negative charge states of the VV_{Si}.

This controversy concerning the VV_{Si} configuration becomes somewhat less crucial when one considers the effect of temperature and the small energetic differences between the proposed configurations. Svensson *et al.*[7] point out that the EPR experiments of Watkins and Corbett[1,2] were performed at $\leq$20 K where the low-symmetry LP structure may be frozen-in, and propose that at temperatures $\geq$30 K there will be thermally activated reorientation of the symmetry plane by electronic bond switching. In their model, the bond switching would take place at such a high rate that a symmetry-breaking relaxation could not occur and the resulting configuration would have D_{3d} symmetry. This is the same symmetry obtained by removing two neighboring Si atoms from the perfect crystal. Moreover, Makhov and Lewis[8] recently reported that there is essentially no energy barrier for the transition between the RB and LP configurations. Many of the above-mentioned authors have made note of the relatively flat energy surface associated with the structure of the VV_{Si}. This is consistent with the results of this study, which indicate that even at low temperatures all the proposed configurations may be populated.

As part of a larger effort to quantitatively model the behavior of radiation-induced defects in Si,[9–11] we have investigated the VV_{Si} using density functional theory. Our goal was to obtain accurate zero-temperature formation energies for the defect in all of its stable charge states and calculate the energies where electronic transitions between charge states occur. These values are compared to experimental data obtained from EPR and deep-level transient spectroscopy (DLTS),[1,2,7,12] and will be used in subsequent multiscale modeling. In the course of formation-energy calculations, the zero-temperature ground-state configurations were determined and will be discussed in the context of the beforementioned controversy. The distinguishing aspect of this study is computational breadth: We have performed converged calculations using nominally 216-, 512- and 1000-atom supercells to extrapolate to infinite-sized supercells.

II. THEORETICAL TECHNIQUES

The density functional theory (DFT) calculations were performed using the Socorro[13] code developed at Sandia National Laboratories. Supercell total energies were obtained using both the local density approximation (LDA)[14] and the PBE (Perdew, Burke, Ernzerhof)[15] formulation of the generalized-gradient approximation (GGA) for electronic exchange and correlation (XC). Norm-conserving pseudopotentials were generated using Don Hamann's GNCPP (Ref. 16) code for the LDA calculations and the Fritz-Haber FHI98PP (Ref. 17) code for the PBE calculations. The methodology used for these defect calculations is similar to that used in a recently published study of the silicon monovacancy.[9] For a more in-depth discussion of the methods, see Ref. 9. The parameters and details specific to this study are outlined below.

The plane-wave basis was determined by the convergence of V_{Si} calculations performed by Wright and published elsewhere.[9] As a result, the plane-wave energy cutoff for

LDA (PBE) was set at 17 (20) Ry, which provided the converged lattice parameter of 10.175 (10.335) bohrs. The electron-density-cutoff was always set to 4× that used for the Kohn-Sham functions. Convergence with respect to k-point sampling was evaluated for each size of supercell and each charge state; {4,4,4} Monkhorst-Pack[18] (n_{MP}=4) parameters for 216-atom supercells, n_{MP}=4 for 512-atom supercells, and n_{MP}=3 for 1000-atom supercells. The electronic temperature was set to 1.887×10^{-3} Ry.

Local energy minimum configurations (LEMC) for a defect were determined as follows. A starting configuration was generated by removing 2 neighboring Si atoms from a nominally 216- or 512-atom cell and perturbing the lattice to remove all symmetries. A standard DFT atomic relaxation proceeded until all atomic forces were less than 5×10^{-5} Ry/bohrs. For the 1000-atom supercells, the LEMC was determined as above with n_{MP}=1 Brillouin-zone sampling. Then, the symmetry group of the LEMC configuration was determined and a symmetrized configuration was used as a starting point for 1000-atom calculations with more dense (n_{MP}=2 and n_{MP}=3) Brillouin-zone sampling. The initial LEMC relaxations were carried out to such an extent that the difference in total energy before and after applying symmetrization is negligible.

The formation energies of the proposed LEMCs discussed in the Introduction (LP, RB, or D_{3d}) are similar enough that for a few of the charge states the assignment of the lowest-energy configuration is ambiguous. However, the ground-state configuration was determined by comparing the formation energies from 510-atom (n_{MP}=2) calculations and choosing the structure with the lowest energy. This determination was done with 510-atom supercells in order to reduce the number of computationally demanding 998-atom calculations. Only the lowest-energy configuration of each charge state was refined with higher k-point sampling and larger supercells.

After the LEMC for each defect charge state and supercell size was obtained, the formation energy was computed using the expression

$$E^f[VV^q_{\mathrm{Si}}] = E_T[VV^q_{\mathrm{Si}}] - n_{\mathrm{Si}}\mu_{\mathrm{Si}} + q(E_V + \Delta_{VBE} + E_F), \quad (1)$$

where E^f is the formation energy, E_T is the total energy for a VV_{Si} in charge state q, n_{Si} is the number of Si atoms in the defect supercell, and μ_{Si} is the Si reference chemical potential and was set equal to the energy per atom of bulk Si obtained from a DFT calculation using the same supercell, pseudopotentials, plane-wave basis, Brillouin-zone sampling, and XC formulation as in the defect calculation. E_F is the Fermi level and E_V is the Kohn-Sham eigenvalue at the valence-band edge (VBE) in the bulk Si calculation. Δ_{VBE} is defined to be the difference between the DFT and measured VBE energies. The value of Δ_{VBE} depends on the formulation of exchange and correlation as well as the pseudopotentials, but is expected to be independent of supercell size. We are not aware of a definitive procedure for computing Δ_{VBE}. The method we have used to estimate its value is discussed at the end of this section.

Earlier studies have defined Δ_{VBE} to be the difference in VBE energies from a bulk and a defect calculation,[19,20] in which case Δ_{VBE} varies with the size and shape of the supercell and becomes zero in an infinite-sized supercell. In addition, there is an underlying assumption that the computed value of the VBE energy in an infinite-sized supercell would be the same as the measured value. Hence, for the time being, we used the before-mentioned provisional estimate based on a comparison with experimental measurements.

For the VV_{Si}, q was found to range from +1 to −2. In calculations where $q\neq0$, a uniform background charge (UBC) was used to remove the infinite electrostatic interaction energy between the VV^q_{Si} and its periodic images.[21] In a separate study by one of the authors, the formation energies of unrelaxed V^{2+}_{Si} were computed in simple cubic 63-, 215-, 511-, 999-, and 1727-atom supercells using two different methods to remove the infinite electrostatic interaction: (1) the UBC method used in this study and (2) the local-moment countercharge (LMCC) method developed recently by Schultz.[22] When the formation energies from the two methods were extrapolated to an infinite-sized supercell, they agreed to within 2 meV demonstrating the consistency of the two methods.[23] A similar level of agreement has also been found by Lento *et al.*[24] in UBC and LMCC calculations for an unrelaxed +2 Si self-interstitial. In the context of the LMCC method, Schultz has noted that Δ_{VBE} has a single value for all point defects in a material obtained using a given exchange-correlation formulation and pseudopotentials.[11] The definition of Δ_{VBE} that we have used in this study is consistent with Schultz's finding.

Formation energies from three sizes of defect supercells (214-, 510-, and 998-atom) were extrapolated to the infinite case via a maximum-likelihood fit to the Makov-Payne formula truncated at the $1/L^3$ term,[25]

$$E^f[VV^q_{\mathrm{Si}};L,n_{MP},E_F] = E^f[VV^q_{\mathrm{Si}};L\rightarrow\infty,E_F] - \frac{\alpha q^2}{\epsilon L} + \frac{A_3}{L^3}. \quad (2)$$

In this formula, $E^f[VV^q_{\mathrm{Si}};L,n_{MP},E_F]$ is the formation energy of a VV^q_{Si} in a supercell of length L obtained using Monkhorst-Pack parameters (n_{MP}) noted previously, $E^f[VV^q_{\mathrm{Si}};L\rightarrow\infty,E_F]$ is the formation energy in an infinitely sized supercell (determined from the fit), α=2.8373 is the Madelung constant for a simple cubic lattice of point charges embedded in a uniform compensating background, ϵ is the static dielectric constant of Si, and A_3 is the coefficient of the $1/L^3$ term (determined from the fit). For consistency, DFT values of ϵ were used in the fits: 12.9 for the LDA and 12.6 for the GGA.[26] For the fit, we assume Gaussian uncertainties where the error in each data point is estimated by the difference in formation energy between maximum Brillouin-zone sampling and the next-lower level of sampling (calculated during k-point convergence). The use of extrapolation to remove errors in the supercell approximation has been successfully used by Lento *et al.*[24] and Castleton *et al.*[27]

The transition energy between two charge states is the value of E_F where their formation energies become equal. For example, the transition between the q and $q+1$ states occurs at an energy

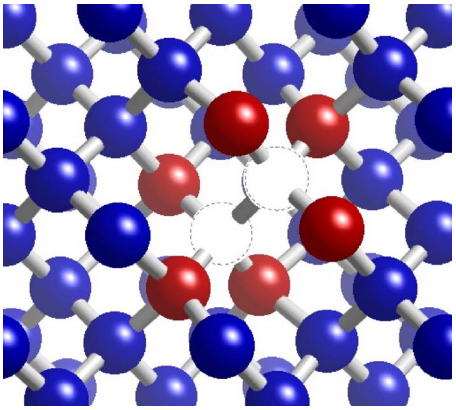

FIG. 1. (Color online) Atomic configuration of the VV_{Si}^{+}. The solid circles represent Si atoms. Dashed circles represent the missing Si atoms. In color, the red solid atoms represent the six Si atoms surrounding the VV_{Si}^{+}.

$$E^{q/q+1} = E^{f}[VV_{\mathrm{Si}}^{q}; L \to \infty, E_F = 0] - E^{f}[VV_{\mathrm{Si}}^{q+1}; L \to \infty, E_F = 0] \quad (3)$$

relative to the VBE. Notice that E_F is set to zero when evaluating the extrapolated formation energies on the right-hand side of this expression. Furthermore, this expression cannot be fully evaluated until a value for Δ_{VBE} is obtained. In this study, Δ_{VBE} was selected to bring a computed transition energy into agreement with a measured value; specifically the $E^{0/1+}$ level, which occurs 0.21 eV above the VBE.[1,2,7,12] Doing so yields $\Delta_{VBE}=-0.329$ for the LDA results and −0.267 for the GGA results. We emphasize that an optimal procedure for computing Δ_{VBE} has not yet been determined and the present approach should be viewed as provisional.

III. RESULTS

In this section we present VV_{Si} LEMCs converged with respect to Brillouin-zone sampling and supercell size. We will then discuss the formation energies from 214-, 510-, and 998-atom defect supercells, which were fit to an extrapolation to obtain formation energies corresponding to infinitely spaced defects. The VV_{Si} has four charge states: singly positive (+), neutral (0), singly negative (−), and doubly negative (−−). The transition energies between charge states and the binding energy for VV_{Si}^{0} were computed and will be compared to experimentally measured values.

The VV_{Si} is created by removing two neighboring Si atoms, which leaves six under-coordinated Si atoms and 18 associated bonds that can accommodate the resulting strain. Because the strain may be distributed over such a large number of bonds, the formation energy of the defect is not sensitive to small changes in the atomic configuration. As a consequence, there are relatively small differences between the formation energies of the LP, RB, and D_{3d} structures.

Figure 1 is a representation of the VV_{Si}. In particular, this is the relaxed ground-state configuration of the + charge state obtained from a calculation with 998 atoms, $n_{MP}=3$, and the PBE functional. Figure 2 is an abstracted view of the VV_{Si} showing the ⟨111⟩ axis of the defect and the surrounding undercoordinated atoms. Triangles can be constructed from the three atoms on each side of the defect. If the defect is viewed along the ⟨111⟩ axis, as shown in Fig. 3, the sense of the Jahn-Teller distortion (LP or RB) can be seen by comparing the relative lengths labeled $d_{1,2}$ and $d_{1,3}$ in the figure. Quantitatively, the LP configuration is characterized by $d_{1,2} < d_{1,3}$, where two of the atoms in each triangle strongly pair [Fig. 3(b)]. The RB configuration is characterized by $d_{1,2}$

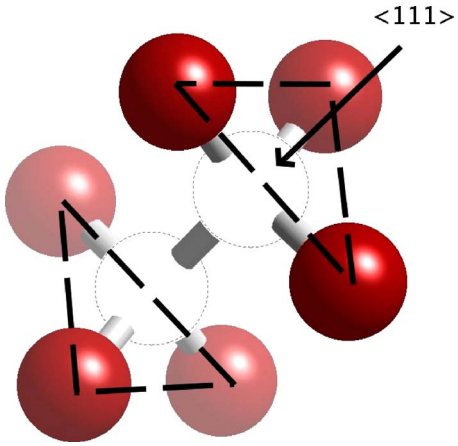

FIG. 2. (Color online) Abstracted view of the VV_{Si} showing only the six atoms surrounding the defect and the missing Si atoms. The axis of the VV_{Si} is along the ⟨111⟩ direction. Solid circles represent the undercoordinated Si atoms surrounding the VV_{Si}. Dashed circles represent missing Si atoms.

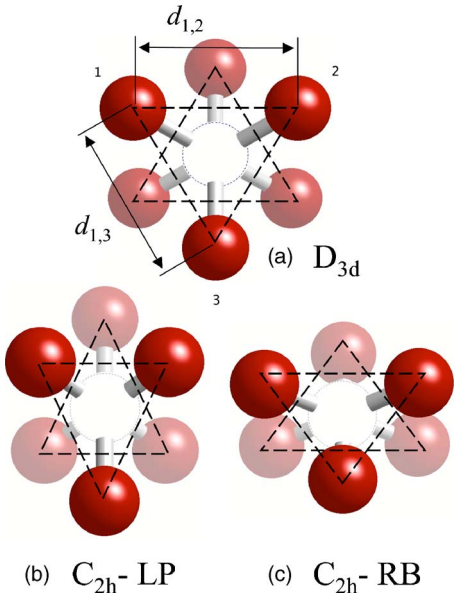

FIG. 3. (Color online) Views of the VV_{Si} rotated so the ⟨111⟩ direction is perpendicular to the plane of the page. (a) The D_{3d} structure where $d_{1,2}=d_{1,3}=d_{2,3}$ involves only a breathing-mode relaxation. (b) The LP structure (C_{2h}) is characterized by $d_{1,2}<d_{1,3}=d_{2,3}$. (c) The RB structure (C_{2h}) is characterized by $d_{1,2}>d_{1,3}=d_{2,3}$. In all three images, $d_{1,3}=d_{2,3}$. Solid circles represent the undercoordinated Si atoms surrounding the VV_{Si}. Dashed circles represent missing Si atoms.

TABLE I. The lowest-energy configuration for each charge state with either LDA or PBE for XC. The energies in parentheses are the difference between the lowest-energy configuration and the other (RB when LP is listed or LP when RB is listed). In the −− charge state, neither the RB nor the LP configuration was found to be a LEMC configuration and therefore no energy difference is listed.

Charge state (q)	LDA	PBE
+	LP (7 meV)	LP (60 meV)
0	RB (15 meV)	LP (1 meV)
−	RB (8 meV)	LP (29 meV)
−−	D_{3d}	D_{3d}

$>d_{1,3}$, where there is a more equitable distribution of bond strain [Fig. 3(c)]. Both of these configurations exhibit the same C_{2h} symmetry. The intermediate case, when $d_{1,2}=d_{1,3}=d_{2,3}$, results in D_{3d} symmetry; In this case there is no symmetry-lowering relaxation and instead a breathing-mode relaxation occurs where the magnitude depends on the particular defect charge state.

The determined ground-state configurations are listed in Table I. Also listed in the table are the differences in energy between the ground-state configuration and the alternate configuration (RB when LP is listed or LP when RB is listed). In several cases, the energy difference between LP, RB, or even D_{3d} is less than 10 meV.

By looking at the symmetry or the relative lengths $d_{1,2}$ and $d_{1,3}$ (Fig. 3), it may appear that there is a drastic difference between the LP, RB, or D_{3d} configurations. However, a 0.5 Å change in length A or B may represent only slight bond bending and a much smaller change in the three near-neighbor bond lengths associated with each atom. In other words, the lengths $d_{1,2}$ and $d_{1,3}$ that characterize the sense and magnitude of the Jahn-Teller distortion do not directly correlate to actual bond lengths. Because the actual bond lengths and angles are only changing slightly, the change in the energy of the defect is correspondingly slight.

In the −− charge state, the symmetry was initially broken (set towards both RB and LP) but the structure relaxed back towards the D_{3d} symmetry. Neither of the C_{2h} symmetry configurations were found to be locally stable for this charge state. For the other three charge states, we additionally constrained the symmetry to D_{3d} and computed the total energy with PBE, 510-atom cells, and $n_{MP}=4$ sampling. The results were then compared to the LP configuration. The structure with D_{3d} symmetry was 63, 169, and 37 meV higher in energy for the +, 0, and − charge states.

TABLE II. Formation energies for VV_{Si} calculated with the LDA. The Brillouin-Zone was sampled using $n_{MP}=4$, $n_{MP}=4$, and $n_{MP}=3$ MP parameters for the 214-, 510-, and 998-atom supercells, respectively. The last row contains values extrapolated to an infinite sized supercell.

Cell size	VV^{+}_{Si}	VV^{0}_{Si}	VV^{-}_{Si}	VV^{--}_{Si}
214	5.481	5.340	5.498	5.627
510	5.368	5.269	5.545	5.777
998	5.298	5.228	5.560	5.843
∞	5.336	5.217	5.635	6.108

TABLE III. Formation energies for VV_{Si} calculated with the PBE. The Brillouin zone was sampled using $n_{MP}=4$, $n_{MP}=4$, and $n_{MP}=3$ MP parameters for the 214-, 510-, and 998-atom cells respectively. The last row contains values extrapolated to an infinite-sized supercell.

Cell size	VV^{+}_{Si}	VV^{0}_{Si}	VV^{-}_{Si}	VV^{--}_{Si}
214	5.486	5.445	5.681	5.786
510	5.415	5.402	5.691	5.952
998	5.383	5.370	5.710	6.032
∞	5.420	5.363	5.801	6.301

Formation energies corresponding to the converged ground-state configurations of each cell size were used to extrapolate to an $L\rightarrow\infty$ value, where L is the length of one side of the supercell. The extrapolation was performed by fitting to the Makov-Payne formula as described in Sec. II. The $L\rightarrow\infty$ formation energies are listed in Table II (LDA) and Table III (PBE).

The changes in formation energy with supercell size indicate that the dependence of the electrostatic interactions between periodically repeated defects is not simply a Madelung term, i.e., linear in $1/L$ where L is the cube root of the supercell volume. Notice also that the formation energies for the neutral defect change with increasing supercell size. This could be due to higher-order electrostatic interactions (quadrupole-quadrupole) or interactions between defect strain fields in the periodically repeated supercells. A more in-depth discussion of strain interactions in periodic bulk defect calculations can be found elsewhere.[9]

Computed energy levels for the transitions between charge states are shown in Fig. 4 where they are compared to experimental values taken from the literature.[1,2,7,12] As discussed in the previous section, Δ_{VBE} was chosen such that the $E^{+/0}$ transition is aligned with the measured value (0.21 eV). The measured values for the $E^{0/-}$ and $E^{-/--}$ transitions are

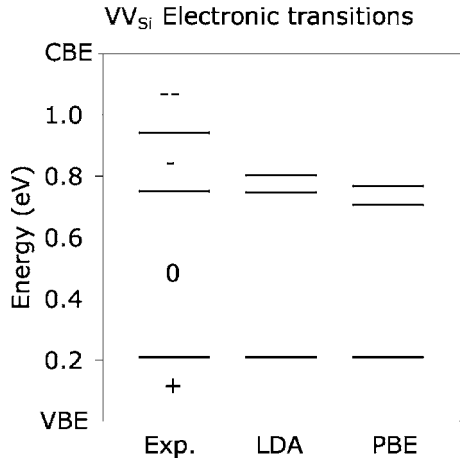

FIG. 4. Calculated electronic transitions between VV_{Si} charge states compared to measured values from the literature.

0.75 and 0.94 eV. The calculated LDA (PBE) transitions are $E^{0/-}=0.75(0.71)$ eV and $E^{-/--}=0.80(0.77)$ eV. The LDA results reproduce the correct spacing between $E^{+/0}$ and $E^{0/-}$, and the PBE results are also in good agreement. However, in this study, neither LDA or PBE quantitatively predict the correct spacing between $E^{0/-}$ and $E^{-/--}$. In order to rule out the possibility that the low predicted values for $E^{-/--}$ were the result of partial occupation of eigenstates in the conduction band, we recalculated the total energy of a 214-atom, PBE, $n_{MP}=4$, VV_{Si}^{--} using a discrete occupation scheme suggested by Schultz.[11] However, compared to our original calculation, the discrete occupation of energy levels changed the total energy by only 2.4 meV.

In a recent LDA study using a Gaussian basis, 248-atom supercells, and $n_{MP}=2$, and the LP structure, Schultz[11] has also predicted the spacings between the $E^{+/0}$, $E^{0/-}$, and $E^{-/--}$ transitions, which qualitatively agree with our results and agree well with experiment.

Binding energies can be calculated from the extrapolated VV_{Si} formation energies and similarly obtained formation energies for the monovacancy[9] using the equation

$$E_B = E^f(V_{\mathrm{Si1}}^{q1}) + E^f(V_{\mathrm{Si2}}^{q2}) - E^f(VV_{\mathrm{Si}}^{q1+q2}), \tag{4}$$

where V_{Si1} and V_{Si2} are the resulting dissociated Si monovacancies, and where $q1$ and $q2$ are the corresponding monovacancy charge states. The most simple case is where $q1=0$ and $q2=0$, since the charge state remains unchanged before and after dissociation. The corresponding $E^f(V_{\mathrm{Si}}^0, L\rightarrow\infty)$ for LDA and PBE are 3.457 and 3.605 eV,[9] which gives binding energies for VV_{Si}^0 of 1.70 (LDA) and 1.85 eV (PBE). These values agree reasonably well with the 1.60 eV (LDA) reported by Pesola *et al.*[5] and the experimentally estimated value of $\geq$1.6 eV.[2] Using the data in Tables II and III, and monovacancy data from Wright,[9] one may calculate binding energies for various values of $q1$ and $q2$.

IV. SUMMARY

Atomic configurations, formation energies, electronic transition energies, and binding energies of VV_{Si}^q were obtained from DFT calculations using norm-conserving pseudopotentials, a plane-wave basis, and both the LDA and PBE formulations of exchange and correlation. Formation energies from supercells containing 214, 510, and 998 atoms were extrapolated to an infinite-sized supercell to remove spurious electrostatic interactions arising from the use of periodic boundary conditions. The atomic structure was found to depend on the defect charge state and the formulation of exchange and correlation. The PBE structures more closely agree with EPR experiments predicting the LP structure with C_{2h} symmetry for the +, 0, and − charge states, but predict the D_{3d} structure for the −− charge state. The LDA calculations predict RB structure with C_{2h} symmetry for the 0 and − charge state, the LP structure for the + charge state, and the D_{3d} structure for the −− charge state. However, because there is only a small difference in formation energies between the two C_{2h} (RB and LP) and also the D_{3d} structure, all of the configurations should be relevant even at low temperature. Computed binding energies, which agree closely with experiment, indicate that monovacancies will react to form strongly bound divacancies if they become mobile.

ACKNOWLEDGMENTS

Sandia is a multiprogram laboratory operated by Sandia Corporation, a Lockheed Martin Company, for the United States Department of Energy's National Nuclear Security Administration under Contract No. DE-AC04-94AL85000. This work was partially supported by Basic Energy Sciences, Office of Science, Division of Materials Science, United States Department of Energy. We would like to acknowledge rewarding discussions with Normand Modine of Sandia National Laboratories.

[1] J. W. Corbett and G. D. Watkins, Phys. Rev. Lett. **7**, 314 (1961).
[2] G. D. Watkins and J. W. Corbett, Phys. Rev. **138**, A543 (1965).
[3] M. Saito and A. Oshiyama, Phys. Rev. Lett. **73**, 866 (1994).
[4] H. Seong and L. J. Lewis, Phys. Rev. B **53**, 9791 (1996).
[5] M. Pesola, J. von Boehm, S. Poykko, and R. M. Nieminen, Phys. Rev. B **58**, 1106 (1998).
[6] S. Ogut and J. R. Chelikowsky, Phys. Rev. Lett. **83**, 3852 (1999).
[7] B. G. Svensson, B. Mohadjeri, A. Hallen, J. H. Svensson, and J. W. Corbett, Phys. Rev. B **43**, 2292 (1991).
[8] D. V. Makhov and L. J. Lewis, Phys. Rev. B **72**, 073306 (2005).
[9] A. F. Wright, Phys. Rev. B **74**, 165116 (2006).
[10] N. A. Modine (unpublished).
[11] P. A. Schultz, Phys. Rev. Lett. **96**, 246401 (2006).
[12] A. O. Evwaraye and E. Sun, J. Appl. Phys. **47**, 3776 (1976); E. V. Monakhov, B. S. Avset, A. Hallen, and B. G. Svensson, Phys. Rev. B **65**, 233207 (2002); M. Stavola and L. C. Kimerling, J. Appl. Phys. **54**, 3897 (1983); M. Asghar, M. Zafar, and N. Zafar, *ibid.* **73**, 4240 (1993).
[13] See http://dft.sandia.gov/socorro
[14] D. M. Ceperley and B. J. Alder, Phys. Rev. Lett. **45**, 566 (1980); J. P. Perdew and A. Zunger, Phys. Rev. B **23**, 5048 (1981).
[15] J. P. Perdew, K. Burke, and M. Ernzerhof, Phys. Rev. Lett. **77**, 3865 (1996).
[16] D. R. Hamann, Phys. Rev. B **40**, 2980 (1989).
[17] M. Fuchs and M. Scheffler, Comput. Phys. Commun. **119**, 67 (1999).
[18] H. J. Monkhorst and J. D. Pack, Phys. Rev. B **13**, 5188 (1976).
[19] S. B. Zhang and J. E. Northrup, Phys. Rev. Lett. **67**, 2339 (1991); D. B. Laks, C. G. Van de Walle, G. F. Neumark, P. E. Blochl, and S. T. Pantelides, Phys. Rev. B **45**, 10965 (1992); J. E. Northrup and S. B. Zhang, *ibid.* **47**, 6791 (1993).
[20] A. Garcia and J. E. Northrup, Phys. Rev. Lett. **74**, 1131 (1995).
[21] Y. Bar-Yam and J. D. Joannopoulos, Phys. Rev. B **30**, 1844 (1984).
[22] P. A. Schultz, Phys. Rev. B **60**, 1551 (1999); Phys. Rev. Lett. **84**, 1942 (2000).

[23] A. F. Wright and N. A. Modine, Phys. Rev. B (to be published).
[24] J. Lento, J.-L. Mozos, and R. M. Nieminen, J. Phys.: Condens. Matter **14**, 2637 (2002).
[25] G. Makov and M. C. Payne, Phys. Rev. B **51**, 4014 (1995).
[26] V. Olevano, M. Palummo, G. Onida, and R. Del Sole, Phys. Rev. B **60**, 14224 (1999).
[27] C. W. M. Castleton, A. Hoglund, and S. Mirbt, Phys. Rev. B **73**, 035215 (2006).